JOURNAL OF GEOPHYSICAL RESEARCH, VOL. 91, NO. B9, PAGES 9447-9451, AUGUST 10, 1986

Global Nondynamic Orbit Improvement for Altimetric Satellites

DAVID T. SANDWELL,[1] DENNIS G. MILBERT AND BRUCE C. DOUGLAS

National Geodetic Survey Division, National Ocean Service, NOAA, Rockville, Maryland

The largest source of error in satellite altimetry is in the radial position of the satellite. Radial orbit errors of more than a few decimeters prohibit basin-scale studies of sea surface height variability. We explore nondynamic techniques for reducing this error. Sea surface height differences at intersections of satellite altimeter profiles (crossover data) provide a strong constraint on radial orbit error but do not uniquely define it. The portion of orbit error that is a function of latitude and longitude only produces no crossover differences and therefore cannot be recovered with crossover data. Using mathematics (inclination functions) originally developed for satellite dynamics, we determine the entire class of orbit error functions not recoverable with crossover data. These functions are mappings of surface spherical harmonics into the orbit plane. For example, the $l=1$, $m=0$ surface harmonic maps into sinusoidal orbit error with a frequency of once per orbit. Nonzonal harmonics map into linear combinations of three or more frequencies that are linked by the inclination functions. Between frequencies of 0 and 2.2 cycles per orbit there are nine orbit error components that cannot be recovered using crossover data. These components are uniquely defined, however, by nine globally distributed radial tracking points. Fewer tracking points are sufficient if a smoothness criteria is applied to the orbit correction curve. Our findings suggest that radial orbit error can be significantly reduced by including a few globally distributed radar reflectors (or transponders) in the tracking network.

INTRODUCTION

Satellite altimetry is a valuable observing technique for geodesists, geophysicists, and oceanographers. For some applications, however, the technique is limited by orbit determination accuracy. The radial component of orbit error introduces a long-wavelength bias (~30 cm currently) into altimeter profiles. This is many times the precision of any recent or future instrument. The dominant portion of this error arises from uncertainty of the earth's gravity field [*Marsh and Williamson*, 1980]. Until knowledge of the geopotential is substantially improved, nondynamical (geometric) orbit determination techniques must be explored. The nondynamic orbit improvement method, presented here, is intended to reduce the small radial orbit errors remaining in precision orbits; it does not replace precision orbit determinations.

Several nondynamic techniques have been developed to reduce radial orbit error. In each case the orbit was adjusted to minimize the differences in sea surface height at intersections of ascending and descending altimeter profiles (i.e., crossover differences). *Rummel and Rapp* [1977] adjusted the bias and trend of each altimeter profile, in a restricted area, to minimize all crossover differences. This method has also been applied to large regions and to a set of "primary arcs" [*Rapp*, 1983], giving global coverage. *Cloutier* [1981] computed the smoothest curve reducing the crossover differences and average radial error to zero. *Wunsch and Zlotnicki* [1984] did not explicitly form crossover differences but regionally modeled radial orbit error using covariance functions in a least squares approach. *Douglas et al.*, [1984] (hereinafter referred to as DAS) used a truncated Fourier series to model the orbit error globally.

All of these investigators found that crossover data alone, no matter how geographically dense, do not uniquely determine radial orbit error. Various methods have been used to stabilize the problem of recovering radial orbit error from crossover data. Regional solutions, where biases and trends were removed from each pass, were stabilized by fixing three points in the area or pinning the edges of the area to the most accurate passes (i.e., master arcs). *Cloutier* [1981] stabilized the problem by seeking the minimal rate of change of orbit error giving an average orbit error of zero. *Wunsch and Zlotnicki* [1984] avoided singularities by prescribing a covariance function for radial orbit error. Finally, DAS overcame the problem by including low-weighted altimetrically determined sea surface heights not at crossover points. While these stabilization methods are practical, it is not clear that they yield an accurate orbit in every case.

The new technique presented here still relies mainly on crossover data. However, it is designed to extract basin-scale oceanographic signals from altimeter profiles and thus must meet several criteria. First, the time span of the corrected orbit should be long enough to create a global map (e.g., one ground track repeat cycle) but short enough that sea surface topography does not change appreciably. Second, it is desirable that sea surface topography from different months, or even years, be compared to determine seasonal or secular variations.

To attain these goals, we first identify all of the components of radial orbit error that are not recoverable from crossover data. It is shown that these unrecoverable components depend on latitude and longitude only. Such purely geographical orbit error produces no crossover differences, so it cannot be recovered with crossover difference data. After identifying these unrecoverable components, we determine the minimum additional tracking data needed to constrain them. In theory, the minimum tracking data along with the crossover data uniquely define the orbit. In practice, data gaps over continental areas destroy this unique relationship. The orbit is poorly constrained over continental areas but is accurate over ocean areas. Thus the improved radial position of the satellite cannot be used to deduce the forces acting on the satellite. Our method only improves the accuracy of sea surface topography.

Several studies have identified Fourier components of orbit error that depend only on latitude and longitude. The mapping of the $l=1$, $m=0$ surface spherical harmonic into once per revolution was found by *Douglas and Sandwell* [1983]. *Wagner* [1985] used a simple argument to show that once per revolution orbit error and all multiples thereof were unobservable from crossover data. He proposed that all the zonal spherical harmonics map into multiples

[1]Now at Center for Space Research, The University of Texas at Austin.

Paper number 5B5725.

of the once per revolution frequency. Here we use inclination functions, developed originally for satellite dynamics [*Kaula*, 1966; *Allan*, 1973], to confirm that the zonal harmonics map into multiples of once per revolution. Furthermore, we show that the nonzonal harmonics map into linear combinations of three or more frequencies. Thus, for each surface spherical harmonic (time independent) there is a component of radial orbit error that cannot be recovered with crossover data.

GEOGRAPHICALLY DEPENDENT RADIAL ORBIT ERROR

The focus of this study is the Fourier model for radial ephemeris error used by *Goad et al.* [1980] in their attempt to improve altimetric satellite orbits on a global scale using crossovers. The orbit error model is

$$O(t) = \sum_{i=0}^{N} a_i \cos(2\pi \omega_i t) + b_i \sin(2\pi \omega_i t) \quad (1)$$

for N frequencies ω_i. There are several advantages to this model. First, there is negligible radial error in a precise ephemeris at frequencies higher than twice per revolution [*Marsh and Williamson*, 1980] so if the Fourier model is truncated near twice per revolution, the number of model parameters is much less than the number of crossover data for arcs more than a few days in length. Second, the correction curve is global but limited in time. This time window is ideal for ocean dynamic studies. Finally, we show the class of geographically correlated orbit error consists of just a few Fourier components. These components can be eliminated from the model, or better, determined from additional data.

Radial orbit error that depends only on latitude and longitude produces no height differences at crossover points. Consider this in the context of the largest single component of orbit error: one cycle per orbit. The sine component (as measured from the equator) of orbit error depends on latitude alone. Latitude is unaffected by earth rotation. Previous studies [*Douglas and Sandwell*, 1983] have shown that it is perfectly correlated with the $l=1$, $m=0$ surface spherical harmonic and is therefore unobservable from crossover data. In contrast, the cosine component of once per revolution orbit error is observable from crossover data because the earth rotates with respect to the orbit plane. When the cosine component of orbit error returns to the same value (after one cycle) the longitude has changed because of earth rotation.

In addition to the mapping of the $l=1$, $m=0$ surface spherical harmonic into the sine component of once per revolution orbit error, there is a similar mapping for every other surface harmonic. The complete set of radial orbit error functions depending only on latitude and longitude is most easily found by projecting individual surface harmonics into the Fourier spectrum of the radial orbit error. These mapping functions were derived originally to compute the earth's gravitational potential along a satellite trajectory [*Kaula*, 1966; *Allan*, 1973]. Here we use the same formulation to map surface harmonics into the orbit plane. For a circular orbit, the mapping of the surface spherical harmonics of degree l and order m (i.e., C_{lm} and S_{lm}) into radial orbit error $O_{lm}(t)$ is

$$O_{lm}(t) = \sum_{p=0}^{l} F_{lmp}(I) \left[A_{lm} \cos(\psi_{lmp} t) + B_{lm} \sin(\psi_{lmp} t)\right] \quad (2)$$

where

$$A_{lm} = \begin{cases} C_{lm} & l-m \text{ even} \\ -S_{lm} & l-m \text{ odd} \end{cases} \qquad B_{lm} = \begin{cases} S_{lm} & l-m \text{ even} \\ C_{lm} & l-m \text{ odd} \end{cases} \quad (3)$$

and

$$\psi_{lmp} = (l-2p)\omega_o + m\omega_e \quad (4)$$

and the $F_{lmp}(I)$ are the inclination functions given by *Kaula* [1966]. Without loss of generality we have chosen $t=0$ at zero latitude and zero longitude. These mappings depend upon the orbit frequency ω_o, the orbit inclination I, and the earth rotation rate relative to the orbit plane ω_e. To determine mappings of individual harmonic coefficients into radial orbit error, two cases must be considered, $l-m$ even and $l-m$ odd. Mapping functions, up to degree and order 2, are listed in Table 1. The odd zonal harmonics (i.e., $l=1,3,5\cdots$; $m=0$) map into sine functions with frequencies of ω_o, $3\omega_o$, $5\omega_o\cdots$, respectively. The even zonals map into cosines of even multiples of ω_o. The nonzonal mapping functions are more interesting since they map into sets of frequencies related through the inclination functions (see Table 1). For example, $C_{1,1}$ maps into two cosine terms with frequencies of $\omega_o \pm \omega_e$; $S_{1,1}$ maps into sine terms having the same frequencies. The superposition of these two sine components is $2\cos(\omega_o t)\cos(\omega_e t)$. This is orbit error with a frequency of once per revolution and amplitude modulated by the earth's rotation rate. Note that these functions have been derived without requiring the orbit to be in a repeat mode.

For a concrete example, consider a Fourier model that is restricted to frequencies between 0 and 1.1 cycles per revolution. The frequency sets that cannot be determined from crossover data are 0, ω_o, and $\omega_o \pm \omega_e$. With respect to crossover data these are singular orbit error components. Higher spherical harmonics such as $l=2$, $m=2$ map into a linear combination of $2\omega_o \pm \omega_e$ and ω_e. Even though ω_e is below 1.1 cycles per revolution, it does not produce a singular component. A singularity only occurs if one attempts to recover all of the components of the linear combination simultaneously. In the subsequent numerical analysis, using the frequency pair $\omega_o \pm \omega_e$, it is demonstrated that $\omega_o + \omega_e$ by itself is not singular; it is only singular in combination with $\omega_o - \omega_e$.

NUMERICAL EXAMPLES

The mapping function in equation (2) was derived for a circular orbit. To estimate the effect of the slight eccentricity of the Seasat orbit, as well as irregular sampling due to land masses, numerical techniques must be used to calculate the actual strength of the singularities. We use the least squares technique but believe other numerical techniques will yield similar results.

Figure 1 shows the results of repeated fitting (least squares) of a one-frequency model (sine and cosine) to the 354 deep water, land-and-ice free Seasat crossover data in the 3-day repeat cycle from September 20–22, 1978, used by DAS. The abscissa displays a selected frequency, and the ordinate displays the condition number of the Euclidian norm (spectral norm) of the normal equation matrix. This condition number is a measure of the conditioning (or singularity) of a system [*Gill et al.*, 1981]. It indicates the maximum effect of a perturbation on an exact solution. The condition number ranges from 1 (completely stable) to infinity (exactly singular). Figure 1 shows clearly the single-frequency singularity at once per revolution. We also found that sharp singularities occur at integer multiples of once per revolution. The extreme sharpness of the singularities is surprising, since the real orbit is not exactly circular and has complex perturbations.

To illustrate the additional singularities arising from combinations of frequencies (i.e., $\omega_o \pm \omega_e$), another condition number computation was performed. Figure 2 shows the

TABLE 1. Mapping Functions

l	m	p	ω	$F_{lmp}(I)$	$F_{lmp}(108°)$ (Seasat)	$S_{lmp}(\omega t)$
0	0	0	0	1	1.00	C_{00}
1	0	0	ω_o	$-\frac{1}{2}\sin I$	0.48	$C_{10}\sin(\omega_o t)$
1	0	1	$-\omega_o$	$\frac{1}{2}\sin I$	−0.48	$-C_{10}\sin(\omega_o t)$
1	1	0	$\omega_o+\omega_e$	$\frac{1}{2}+\frac{1}{2}\cos I$	0.35	$C_{11}\cos(\omega_o+\omega_e)t - S_{11}\sin(\omega_o+\omega_e)t$
1	1	1	$-\omega_o+\omega_e$	$\frac{1}{2}-\frac{1}{2}\cos I$	0.65	$C_{11}\cos(\omega_o-\omega_e)t + S_{11}\sin(\omega_o-\omega_e)t$
2	0	0	$2\omega_o$	$-\frac{3}{8}\sin^2 I$	−0.34	$C_{20}\cos(2\omega_o t)$
2	0	1	0	$\frac{3}{4}\sin^2 I-\frac{1}{2}$	0.18	C_{20}
2	0	2	$-2\omega_o$	$-\frac{3}{8}\sin^2 I$	−0.34	$C_{20}\cos(2\omega_o t)$
2	1	0	$2\omega_o+\omega_e$	$\frac{3}{4}\sin I\,(1+\cos I)$	0.49	$S_{21}\cos(2\omega_o+\omega_e)t + C_{21}\sin(2\omega_o+\omega_e)t$
2	1	1	ω_e	$-\frac{3}{2}\sin I\cos I$	0.44	$S_{21}\cos(\omega_e t)+C_{21}\sin(\omega_e t)$
2	1	2	$-2\omega_o+\omega_e$	$\frac{3}{4}\sin I\,(1-\cos I)$	0.93	$S_{21}\cos(2\omega_o-\omega_e)t - C_{21}\sin(2\omega_o-\omega_e)t$
2	2	0	$2\omega_o+2\omega_e$	$\frac{3}{4}(1+\cos I)^2$	0.36	$C_{22}\cos(2\omega_o+2\omega_e)t - S_{22}\sin(2\omega_o+2\omega_e)t$
2	2	1	$2\omega_e$	$\frac{3}{2}\sin^2 I$	1.35	$C_{22}\cos(2\omega_e t)-S_{22}\sin(2\omega_e t)$
2	2	2	$-2\omega_o+2\omega_e$	$\frac{3}{4}(1-\cos I)^2$	1.29	$C_{22}\cos(2\omega_o-2\omega_e)t + S_{22}\sin(2\omega_o-2\omega_e)t$

condition number for a pair of frequencies (four unknowns) using the same 354 crossover data set of DAS. The frequencies were selected by adding and subtracting an offset to the orbital frequency ω_o. The peak of the singularity, associated with the nonzonal harmonic $l=1$, $m=1$, is offset by the rotation frequency of the earth relative to the precessing orbit plane ω_e as predicted by the theory.

To show the behavior of singularities in the full Fourier model used by DAS, we solved for Fourier components (equation (1)) at the following frequencies:

$$N = 93$$
$$\omega_i = i * \omega_1 \quad (i = 0, 1, 2, \cdots, N) \tag{5}$$
$$\omega_1 = \frac{1}{43} \text{ cycles per revolution}$$

A numerical test of this system revealed the expected singularities at once and twice per revolution and also at frequencies $\omega_o \pm \omega_e$, $2\omega_o \pm \omega_e$, and $2\omega_o \pm 2\omega_e$ as predicted from the theory.

Having identified the complete set of orbit error functions not recoverable from ocean crossover data, we also considered the case of complete global sampling, of course obtaining the same result. Obviously, additional information is required if a solution to the orbit error problem is to be obtained.

Inclusion of Additional Data

To provide a formal measure of the effectiveness of including additional data in a generalized least squares solution, a synthetic altimeter orbit error data set was created by subtracting the radial ephemeris component computed by the Goddard Space Flight Center (GSFC) from the radial component of the ephemeris computed by the Naval Surface Weapons Center (NSWC). This yielded 89,081 over water, once per second orbit error values for the period September 20–22, 1978. Data more than one eighth of a revolution from a crossover point were omitted. Of course, any orbit error common to both ephemerides will not appear in these

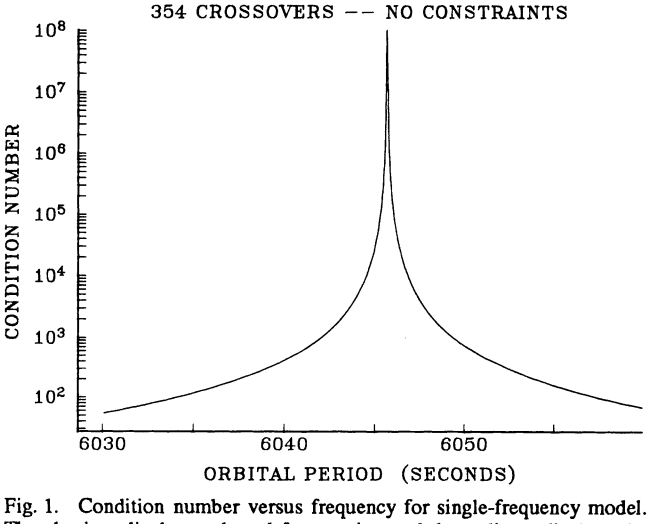

Fig. 1. Condition number versus frequency for single-frequency model. The abscissa displays selected frequencies, and the ordinate displays the condition number of the Euclidian norm (spectral norm) of the normal equation matrix.

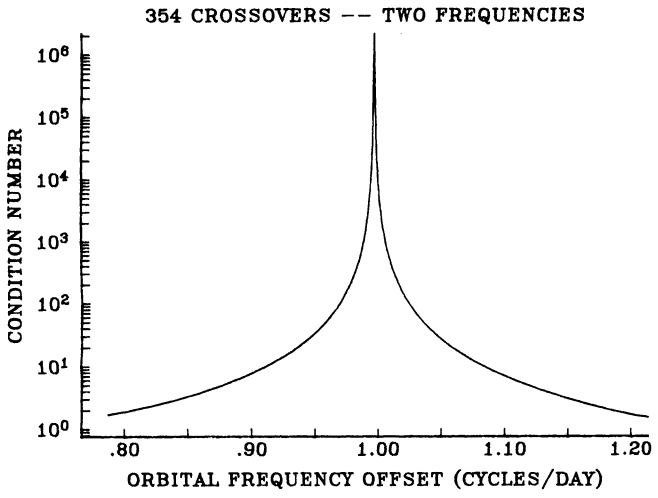

Fig. 2. Condition number for frequency pairs surrounding orbit frequency. The condition number is for the normal equations for a pair of frequencies (four unknowns) using the 354 crossover data set of DAS. The frequencies were selected by adding and subtracting an offset to the orbital frequency.

synthetic data. But since the two ephemerides were derived using different tracking systems and force models, it is implausible that their errors would be exactly in phase.

The synthetic orbit error possessed an uncorrected, root mean square (rms) amplitude of 1.92. The magnitude of the synthetic error was halved to more nearly represent the accuracy of newer Seasat orbits. This yielded an uncorrected rms of 0.96 for the 89,081 points in the 3-day set. From these data a set of 354 synthetic crossover differences were generated. They have uncorrected crossover rms of 1.09 and the time sampling corresponding to the data set used by DAS. Note that if the error had no geographic correlation, the crossover difference rms would have been $\sqrt{2}$ times the orbit error rms.

We used all of the crossover data and a varying number of additional constraints to recover the synthetic orbit error. The constraints were assigned standard deviations of 0.1 m and were globally distributed. The orbit error was modelled as a Fourier series with 90 frequencies. Frequencies were evenly spaced between zero and slightly more than twice per revolution. The theoretical analysis, presented above, predicts this system of linear equations has a rank deficiency of 7.

The results shown in Table 2 reveal the importance of constraining the orbit in just a few places. When one constraint is used, the rms crossover difference is reduced from 1.09 m to 0.064 m. However, the rms orbit error increases from 0.96 m to more than 9 km. A plot of this large orbit error shows that it matches the $l=1$, $m=0$ spherical harmonic. Orbit error is zero at the equator, positive in the northern hemisphere and negative in the southern hemisphere. The error is reduced to 61 m when three constraints are used. When eight constraints are used the error is reduced to 0.36 m. Note the number of constraints has little effect on the rms of the crossover differences. This simulation shows that ocean crossover data and a few globally distributed constraints uniquely define the orbit over ocean areas. The orbit is inaccurate over continental areas, however. This is why we did not consider data more that one eighth of a revolution from a crossover point in this simulation.

In practice it will be difficult to obtain globally distributed unbiased altitude constraints of such high precision. One practical method is to use altimeter ranges from accurately located reflectors as constraints. Radar reflections from the sea surface are precise, but the surface must first be accurately positioned in a geocentric coordinate system. Then variations in sea surface height must be monitored to the same high accuracy, perhaps with an inverted echo sounder [*Miller et al.*, 1985] or other instrumentation. It may be easier to use inland lakes and salt flats as reflectors. They could be accurately positioned using modern geodetic techniques. The levels and tilts of the lakes could then be monitored with tide gauges. Once the reflective surfaces are established, they will provide reference points for calibrating both the orbit and altimeter ranges for many years. While many technical details must still be addressed, the ability to reduce radial orbit error using crossover differences and just a few absolute altitude constraints is appealing.

SMOOTHNESS CRITERIA

Another form of information that can be used is to require the orbit correction curve to be smooth. That is, the integral of the square of the slope of the correction curve should be minimal. This criterion reflects our knowledge that the power spectrum of radial orbit error decreases with increasing frequency above 1 cycle per revolution. This concept has been developed into an orbit improvement method by *Cloutier* [1981]. He solved a function

$$\min \quad \Phi = \sum_{i=1}^{n} W_i \, (O_{i+1} - O_i)^2 \tag{6}$$

for orbit error O_i at time t_i for a given weight W_i,

$$W_i = \frac{1}{t_{i+1} - t_i} \qquad W_i = \frac{1}{(t_{i+1} - t_i)^2} \tag{7}$$

subject to constraints that all crossover differences are zero.

We also have developed a smoothness criterion to select among an infinite number of possible solutions. Our technique does not require that all of the crossovers are zero. Instead the crossover minimization competes with the smoothness criteria. We solve the function

$$\min \quad \Phi = \sum_{i=1}^{n} W_c \Delta_i^2 + \sum_{k=1}^{m} W_s \left[\frac{\Delta O_k}{\Delta t_k} \right]^2 \tag{8}$$

where W_c is the weight on the crossover difference Δ_i and W_s is the weight assigned to the smoothing. The term on the left is the standard form for least squares. The term on the right is the smoothness constraints. Here we recast (8) in the Fourier domain. In the limiting case,

$$\lim_{\Delta t \to 0} \sum_{k=1}^{m} W_s \left[\frac{\Delta O_k}{\Delta t_k} \right]^2 = \frac{1}{T} \int_0^T W_s \left| \frac{dO}{dt} \right|^2 dt \tag{9}$$

We will assume that the orbit error is band limited so it can be expanded in a Fourier series.

$$O(t) = a_o + \sum_{n=1}^{N} a_n \cos(2\pi \omega_n t) + b_n \sin(2\pi \omega_n t) \tag{10}$$

The derivative of $O(t)$ is

TABLE 2. Solutions, 10-cm Constraints

Number. of Altitude Constraints	Crossover rms, m	Orbit rms, m
1	0.064	9138.162
3	0.065	60.532
4	0.065	14.223
8	0.066	0.360

Unfitted subset orbit rms = 0.959 m.

TABLE 3. Gapped Smoothing

Number of Altitude Constraints	Crossover rms, m	Subset Orbit rms, m
1	0.069	3.108
3	0.070	0.303
4	0.070	0.211
8	0.070	0.189

$$\frac{dO}{dt} = \sum_{n=1}^{N} 2\pi\omega_n b_n \cos(2\pi\omega_n t) - 2\pi\omega_n a_n \sin(2\pi\omega_n t) \quad (11)$$

By Parseval's theorem [*Bracewell*, 1978, p. 413] the integral of the square of the orbit slope is

$$\int_0^T \left|\frac{dO}{dt}\right|^2 dt = T \sum_{n=1}^{N} \left[(2\pi\omega_n)^2 a_n^2 + (2\pi\omega_n)^2 b_n^2\right] \quad (12)$$

This allows us to restate our problem in the frequency domain as

$$\min \Phi = \sum_i W_c \Delta_i^2 + W_s T \sum_{n=1}^{N} (2\pi\omega_n)^2 (a_n^2 + b_n^2) \quad (13)$$

The term on the right represents the weighted constraints that stabilize our least squares solution. To achieve a smooth correction curve, the high frequencies are minimized more than the low frequencies. Since we are using a Fourier model for orbit error, the weighted constraints are easily implemented by adding weights $W_s * (2\pi\omega_n)^2$ to the diagonal elements of the normal equation matrix.

The use of smoothing provides some very intuitive results. If the weight on the crossovers W_c is much greater than the weight on the smoothing W_s, then very little information is added to the system of equations. The solution will yield the regular crossover result but with the singular frequencies constrained to zero. On the other hand, if the weight W_c is much less than W_s, then the smoothing predominates. This yields the smoothest solution possible, a flat line.

As a refinement to smoothing, consider the nature of orbit error. As discussed earlier, error in satellite ephemerides is largely concentrated at the orbital frequency. If we had to hypothesize on the appearance of the orbit in the absence of data, we would want it to be smooth except at the orbital frequency. That is, we desire our solution to converge to a once per revolution sinusoid instead of a flat line as data are removed. This refinement is implemented by putting a "gap" in our weighting function at once per revolution so no weight is applied at the orbit frequency. This is equivalent to stating that the orbit is smooth except for a strong (nonzero) signal at once per revolution.

Using gapped smoothing, the results were recomputed and are displayed in Table 3. The use of crossovers plus smoothing gives good results with fewer constraints. This is important since it will be difficult to obtain altitude constraints.

While the results in Table 3 are encouraging, they still illustrate the need for absolute altitude constraints on the orbit. One measurement of the radial orbit error at a point is needed to establish the constant orbit bias a_o. A second measurement is needed to overcome the once per revolution singularity. A few more measurements may be desired, depending upon the smoothness of the orbit and the weight assigned to the smoothing.

SUMMARY

We have developed a technique for reducing radial orbit for altimetric satellites. We first determined the components of radial orbit error that cannot by recovered using crossover data. Each of these singular components is a mapping of a surface spherical harmonic into the orbit plane. For example, the $l=1$, $m=0$ surface spherical harmonic maps into sinusoidal orbit error with a frequency of one cycle per orbit period. The nonzonal harmonics map into linearly dependent sets of $l+1$ frequencies that are related by the inclination functions. Using Seasat crossover data, we demonstrate that the singularities associated with these mappings are extremely sharp.

The theory implies that low frequency (<2 cycles per revolution) orbit error can be uniquely recovered with crossover data and a few globally distributed radial tracking data. Using a numerical example, we confirm that this theory also applies to irregularly spaced data by accurately recovering realistic orbit error using ocean crossover data and eight globally distributed radial tracking data. As expected, the recovered orbit is inaccurate over the continental areas where there is no crossover data.

Considering that forces acting on a satellite are smooth, we also recover the smoothest orbit error function that is consistent with the data. Fewer radial tracking data are required when the smoothness criterion is used. Our findings suggest that a few globally distributed radar reflectors (or radar transponders) should be deployed during altimeter missions to reduce radial orbit error.

Acknowledgments. We thank Carl Wagner for pointing out that the inclination functions could be used to map spherical harmonics into the orbit plane. This work was supported by the National Geodetic Survey and The University of Texas at Austin.

REFERENCES

Allen, R. R., Satellite resonance with longitude-dependent gravity, III, Inclination changes for close satellites, *Planet. Space Sci., 21*, 205–225, 1973.

Bracewell, R. N., *The Fourier Transform and Its Applications*, pp. 444, McGraw Hill, New York, 1978.

Cloutier, J. R., A new technique for correcting satellite ephemeris errors indirectly observed from radar altimetry, *Tech. Rep. TR 246*, Nav. Oceanogr. Office, Bay St. Louis, Miss., 1981.

Douglas, B. C., and D. T. Sandwell, Reduction of radial orbit error by crossover minimization, *Eos Trans. AGU, 64*, 677, 1983.

Douglas, B. C., R. W. Agreen, and D. T. Sandwell, Observing global ocean circulation with Seasat altimeter data, *Mar. Geod., 8*, 67–83, 1984.

Gill, P. E., *Practical Optimization*, p. 401, Academic Press, New York, 1981.

Goad, C. C., B. C. Douglas, and R. W. Agreen, On the use of satellite altimeter data for radial ephemeris improvement, *J. Astron. Sci., 28*, 419–428, 1980.

Kaula, W. M., *Theory of Satellite Geodesy*, p. 37, Blaisdell, Waltham, Mass., 1966.

Marsh, J. G., and R. G. Williamson, Precision orbit analysis in support of the Seasat altimeter experiment, *J. Astron. Sci., 27*, 345–369, 1980.

Miller, L., D. R. Watts, and M. Wimbush, Oscillations of dynamic topography in the eastern equatorial Pacific, *J. Phys. Oceanogr., 15* (12), 1759-1770, 1985.

Rapp, R. H., The determination of geoid undulations and gravity anomalies from Seasat altimeter data, *J. Geophys. Res., 88*, 1552–1562, 1983.

Rummel, R., and R. H. Rapp, Undulation and anomaly estimation using Geos-3 altimeter data without precise satellite orbits, *Bull. Geod., 51*, 73–88, 1977.

Wagner, C. A., Radial variations of a satellite due to gravitational errors: Implications for satellite altimetry, *J. Geophys. Res., 90*, 3027–3036, 1985.

Wunsch, C., and V. Zlotnicki, The accuracy of altimetric surfaces, *Geophys. J. R. Astron. Soc., 78*, 795–808, 1984.

B. C. Douglas and D. G. Milbert, National Geodetic Survey Division, National Ocean Service, NOAA, Rockville, MD 20852.

D. T. Sandwell, Center for Space Research, The University of Texas at Austin, Austin, TX 78712.

(Received July 15, 1985;
revised January 29, 1986;
accepted April 15, 1986.)